Advances in Aerospace Science and Technology, 2022, 7, 146-174
https://www.scirp.org/journal/aast
ISSN Online: 2473-6724
ISSN Print: 2473-6708

Thermodynamic Interpretation of Electron Density and Temperature Description in the Solar Corona

Daniel B. Berdichevsky[1,2,3], **Jenny M. Rodríguez Gómez**[3,4]

[1]College Park, MD, USA
[2]IFIR/UNR-CONICET, Rosario, Sta Fé, Argentina
[3]NASA Goddard Space Flight Center, Greenbelt, MD, USA
[4]The Catholic University of America, Washington, D.C., USA
Email: berdichevsky@ifir-conicet.gov.ar, rodriguezgomez@cua.edu

How to cite this paper: Berdichevsky, D.B. and Gómez, J.M.R. (2022) Thermodynamic Interpretation of Electron Density and Temperature Description in the Solar Corona. *Advances in Aerospace Science and Technology*, **7**, 146-174.
https://doi.org/10.4236/aast.2022.73010

Received: August 2, 2022
Accepted: September 27, 2022
Published: September 30, 2022

Abstract

We reach a thermodynamic interpretation of the CODET model and its accurate electron density and temperature prediction, grounded on the physics of hydro magnetism in global equilibrium. The thermodynamic interpretation finds consistency with the model of a magneto-matter medium possessing a 3-D Langmuir structure. That medium is diamagnetic in the context of ideal magnetohydrodynamic (MHD). It is shown that this magneto-matter has unusual characteristics consistent with assuming that the low quiescent solar corona possesses a nature-state, non yet studied. It is further noticed that this is wholly consistent with the CODET model prediction of a polytropic anomalous index for the electron gas of the Sun's corona. Constitutive properties are derived from this novel state of nature, like magnetic permeability properties and non-dispersive acoustic speed. This non-dispersive acoustic speed is also expected to predict the observed equilibration time for the 1.1 to $1.3R_\odot$ quiescent corona during the solar minimum from 2008 to 2009.

Keywords

Solar Corona, Density, Temperature and Polytropic Anomalous Index

1. Introduction

The Solar corona is the most external layer of the Sun. The solar corona observed in the white-light has three components: the K-corona, related to the solar photospheric light scattered by electrons (dominating at $h \precsim 0.3R_\odot$) the

L-corona consisting of spectral line emission from highly ionized atoms (at $h \precsim 0.5R_{\odot}$) and the F-corona or zodiacal light which presents absorptionlines of the photospheric Fraunhofer spectrum caused by diffraction from interplanetary dust ($h \succsim 0.5R_{\odot}$). They have been observed from the ground during eclipses and from space at distances as small as 0.3 astronomical units to the Sun. In the solar stratified atmosphere, the electron density (or gas pressure) falls off exponentially with height, while the temperature increases reaching more than 1 million K (Howard *et al.* 2019 [1]; Aschwanden, 2019 [2] and 2006 [3]). Where "*h*" is a high with its origin measured vertically and away from an imaginary spherical surface defined by the photosphere surface.

We propose a relatively simple schema for predicting the temperature and density of electrons in the solar corona, specifically in the "K-corona" (Berdichevsky *et al.* 2022 [4], 2020 [5]). On the other hand, earlier the work of Rodríguez Gómez *et al.* 2018 [6] showed how the COronal DEnsity and Temperature (CODET) model describes qualitative the K-corona over more than 11 years (solar cycles 23 and 24). These results illustrate potential contribution to the understanding of the Sun corona, at least under specific conditions.

When we consider the fundamental questions raised in Withbroe, 1988 [7]: "The physical conditions in the Sun corona are vital to the development of an understanding of the mechanisms which heat the coronal plasma; but exists uncertainty of these mechanisms. Additionally, some models ignore the effects of the inward flow of energy carried by thermal conduction from the hottest layers of the corona. As well as the effects of radiative losses in the low corona and chromosphere, corona, transition region." These statements, at least in part, sound true today. There are gaps, especially regarding a lack of understanding when it comes to the high temperature (more than 10^6 K) of the Sun Corona region starting possibly after the transition region (TR) above/near the chromosphere height, and up in altitude to a few solar radii, away from which it is understood that there begins the convection of matter and magnetic field. It likely develops the slow solar wind (SW), see e.g. Sanchez-Diaz *et al.* 2016 [8], Vasquez *et al.*, 2017 [9], moving away from the Sun in its travel of near 100 AU or more until its encounter with the local interstellar medium (LISM, as it is explored in-situ, see e.g., Burlaga *et al.*, 2013 [10], Richardson *et al.*, 2017 [11], Cummings *et al.*, 2016 [12]). However, the role of the magnetic topology, acceleration, energy deposition and heating mechanisms in the solar atmosphere are open questions.

This state of affairs is possibly so despite the much learned on small-scales, as well as the solar network scale: 1) Helioseismology, see e.g., Zhao, Kosovichev, Sekii, 2010 [13]; 2) Nano-flares, see e.g., Klimchuk *et al.*, 2006 [14]; 3) Resolving some of the scales of spicules normal and type II, see e.g., De Pontieu *et al.*, 2007 [15]; 4) Plasma-jets discovery, e.g., Raouafi *et al.*, 2016 [16]. Progress has been immense in our ability to collect solar data with a higher spatial and temporal resolution, see e.g., the high speed/resolution movies of energetic processes identified in the polar magnetic coronal holes of the Sun at their boundaries, which could be connected to a study by Zurbuchen, Schwadron and Fisk, 1997 [17]. This work identified the motion of magnetic field lines foot points proposed previously by Fisk, 1996 [18].

Summing up, it can be said that over the last decades, there has been noticed progress on the physical processes that most likely determine the observed properties of the Sun atmosphere/corona and their outward propagation phenomena (SW, Coronal Mass Ejections, current/plasma sheet). However, these models are valid only if they can account for fundamental properties of the plasma, electron temperatures, electron and ion densities, flow speeds, and magnetic field strength and direction. Unfortunately, these measurements are not known well for long periods like a solar cycle.

Despite this, N_e and T_e can be inferred from remote sensing images of the inner corona and in-situ measurements in the interplanetary medium. When these models are compelling, e.g., Rodríguez Gómez, 2017 [19], they require further understanding of the underlying physics. In this work, we attempt to fill the gap for the simplest case scenario, *i.e.*, the quiescent solar corona.

Then, the extension in time of the quiescent conditions measured in our approach suggests us that the consideration of thermal equilibrium can be physically valid. We proceed to exploit this assumption to infer a consistent, ensemble-based/statistical mechanics approach to describe properties of the plasma. The CODET model provides temperature and number per cubic cm of plasma particles. They are possibly equal to approximately 3/2 to 9/5 of the number of electrons. We consider it reasonable to expect that more than 80% of the ions are likely protons. In this sense, we concentrate on the properties of the K-corona.

In Section 2, we present the thermodynamic interpretation of the CODET model, testing its ability to predict T_e and N_e for the low coronaquantitatively. The thermodynamic interpretations further provide insight through their implications to the plasma properties in the region of the Sun corona. Section 3 touches on the crucial subject of the quiescent solar corona temperature conditions, brought to attention by our *steady-state magneto–matter* interpretation. Section 4 describes the unusual state of matter in the solar corona. Discussion and conclusions are drawn in Sections 5 and 6.

2. Thermodynamic Interpretation

Berdichevsky *et al.* 2022 [4] and 2020 [5] show that the CODET model represents a valuable proxy capable of empirically describing the steady presence in the corona of high temperature and the quantitative estimate of the plasma density with a narrowly constrained uncertainty. In this context the CODET model is capturing properties almost exclusively characteristic of the quiescent solar corona in a region from $1.1 < r/R_\odot < 1.3$. Here, *r* is the distance from the center of mass of the Sun. It is assumed for all purposes to coincide with its geometric center $R_\odot = R = 7 \times 10^5$ km, corresponding to the average location of a relatively *thin* photosphere, about 1000 km thickness, see e.g., in Vernazza, Avrett, and Loeser, 1981 [20]. The CODET model parameters used are listed in the first part of Berdichevsky *et al.*, 2022 [4].

Assuming then an ideal gas of electrons in the corona, the identity connecting electrons number N_e and T_e to the *B*-field magnitude is identified as

$$N_e = B^2 \beta / \left(16\pi \mu k_B T_e\right) \tag{1}$$

where

$$\beta = p \bigg/ \left(\frac{1}{4\pi} B^2 / 2\mu\right) \tag{2}$$

It is assumed that the quiescent Sun corona medium at each altitude layer is constant, as well as the stratification in altitude $h = \left(r - R_\odot\right)$. In this way

$$\beta / 16\pi \mu K_B T_e = f\left(B\right) \tag{3a}$$

and

$$\left(16\pi \mu K_B N_e\right) / \beta = g\left(B\right) \tag{3b}$$

They are valid, *i.e.*, simple relationships with $f(B) = CtB^{2-\zeta}$ and $g(B) = CtB^{2-\alpha}$. where Ct is a constant. Notice that the empirical values for N_e and T_e when it uses the vacuum permeability μ_0 implies a plasma $\beta = 2.5 > 1$.

*A*ssumptions expressed in Equations (3) are explored in the model by using the measured photosphere *B*-field magnitude extrapolated to the location in the corona where electrons T_e and N_e are extracted producing estimates within an uncertainty of about 20% and 30% respectively (see Berdichevsky *et al.*, 2020 [5]). From Equations (1) to (3) we arrive at the presented expressions

$$N_e = B^\xi / Ct_1 \quad \text{and} \quad T_e = B^\alpha / Ct_2 \tag{4}$$

The step-by-step details are given in Rodríguez Gómez, 2017 [19], Rodríguez Gómez *et al.*, 2018 [6]. In Equation (4) Ct_1 and Ct_2 are constants. The model gives an altitude ($r - R_\odot$) dependence for T_e and N_e when the assumptions presented in Equations (1) to (3) are used.

A Possible Interpretation of the Model Polytropic Index *γ*

First, we notice from Equation (4), that the relationship found in the empirical model of Rodríguez Gómez, 2017 [19], connecting temperature and density of the electrons in the corona is

$$N_e \propto T_e^{\gamma - 1} \tag{5}$$

where the thermodynamic parameter γ is for an ideal gas adiabatic process (electrons in this case). It is a simple parameter that depends on the model value of ζ and α as shown in **Appendix 1**. Then the relationship from Equation (5) appears valid from the parameters in **Table 1** Berdichevsky *et al.*, 2022 [4] and Figures in Berdichevsky *et al.*, 2020 [5]. They adequately describe the electrons number (N_e) and temperature (T_e) for a substantial part of the Sun corona, extending from about 1.16 to $1.23 R_\odot$.

Table 1. Magneto-matter constant values result from the thermodynamic interpretation considering a microcanonical statistical mechanical ensemble of magneto–matter homogeneous tubes and their dimensions.

Parameter	Value
Assumed specific heat index C_v	3 kT
Rounded adiabatic polytropic index γ	1/6
Rounded e-gas work coupling constant η	5/4
Rounded ensemble #of magneto-matter tubes	10^{13}
Estimated magneto-matter tubes mean diameter length l	20 km
Estimated magneto-matter tubes mean cross section $\pi(l/2)^2$	314.16 km^2
Estimated magneto-matter tubes mean volume πl^3	25132.74 km^3
Estimated mean number of moles per-magneto-matter tubes	$947221 \equiv 10^6$
Ideal gas-constant R	8.3144598 (48) J mol^{-1} K^{-1}
Gravitational constant G	6.67408 (31) × 10^{-11} m^3 kg^{-1} s^{-2}
Expansion scaling value $¢ = l/R_{\odot}$	2/7 × 10^{-4} (See **Appendix 3**)
V_s (Acoustic, non-diffractive mode)	2 × 10^3 km/s

It is relevant then to point out that Equation (5) identifies an adiabatic condition where an ideal gas is subjected to a thermodynamically reversible process, while entropy (S) is preserved. However, the relationship needed to describe qualitatively the Solar corona observations, Rodríguez Gómez, 2017 [19], requires $\gamma \simeq 1/2$, while the quiescent corona solar minimum CODET model, see **Table 1** values for α and ζ, imposes a $\gamma \simeq 1/6$. Both values of the polytropic index are smaller than one. Therefore, Equation (5) describes an adiabatic process when the gas density decreases and the gas heats up (*i.e.*, $\gamma < 1$).

In addition, notice that for the above obtained γ, following the derivation in Section 2 in Berdichevsky and Schefers, 2015 [21], we found that the anomalous polytropic index $\gamma = 1/2$ corresponds to a parameter $\eta = 7/4$. That is the coupling factor between the competing e-gas pressure and magnetization works. Therefore, the present case $\gamma = 1/6$ corresponds to a coupling parameter 5/4 of the magnetization work to the e-gas work (See derivation in **Appendix 1** and the listed values in **Table 1**).

Next, we proceed to discuss how our interpretation of a *magneto-matter-corona structure* is consistent with the empirical relation identified in Berdichevsky *et al.* 2022 [4] for the description of the quiescent "low" sun corona considering that the relationship from Equation (5), *i.e.*, $N_e \propto T_e^{\gamma-1}$ appears valid.

It will require a theoretical interpretation. We develop a description to explain a diamagnetic condition consistent with the above assumed polytropic $\gamma < 1$ in the Sun Corona. While $|\mathbf{B}|$ changes are at most a factor among photosphere and the low Sun's corona, particles number for this likely fully ionized medium goes from $N \sim 10^{15}$ at $R_{\odot}$ to $\sim 10^{8}$ at $r \sim 1.1 R_{\odot}$ and even less at solar minimum as **Table 1** shows. However, while N_e decreases the T_e increases in a comparable order of magnitude (see low corona T_e in Berdichevsky *et al.* 2020 [5], Figure 3). Therefore, considering the conditions of the medium to be in thermal equilibrium in the region, we proceed to drop the sub-index "*e*" from the temperature "*T*".

This study was constrained to remote sensing inferences only. Such a situation introduces higher uncertainties both in observation and interpretation (see, Berdichevsky *et al.*, 2022). Because the properties of the medium associated with *γ*, substantially smaller than 1, cannot be explored in-situ. Since the materials we used for observations are heat conductors, they do not resist the destructive effect of the observed temperature/radiation so much close the Sun's photosphere/chromosphere.

3. From the Single Electron to an Ensemble of Homogeneous *Magneto-Matter* Regions *in Thermal Equilibrium*

Consider the single electron's Hamiltonian (see e.g., Eq. 89, sect. 41 in Dirac, 1967 [22])

$$H_e = \frac{1}{2} p^2 / m_e + G m_e M_{Sun} \left[r - \langle r \rangle \right] / \langle r \rangle^2 + \boldsymbol{B}(r) \cdot \boldsymbol{m}_e \tag{6}$$

where $\boldsymbol{B} = \mu \boldsymbol{H}$, and here the magnetic permeability μ is a property of the medium to be determined.

Equation (6) provides a synthetic explanation for the possibility that the matter of the Sun Corona far from the Sun does not cool in our extended range in h (height above the photosphere) of the present study, and even far higher, up to a few solar radii. Equation (6) shows that when the electron is higher in the Corona, *i.e.*, $\left[r - \langle r \rangle \right] > 0$, it gains potential energy, which will be equal to the kinetic energy lost in the absence of a magnetic field or another force-field. Now, considering the correct interpretation of the CODET model in the magnetic field $\boldsymbol{B}(r)$ in the Corona, as well as our well-supported understanding of its decrease with increasing *r*, the effect may result in a net increase of kinetic energy by the electron in Equation (6).

Hence, we assume that the gravitational and magnetic fields are such that a net increase in the electron's kinetic energy takes place. We also assume that in the region of the quiescent Corona, there is a global thermodynamic equilibrium, *i.e.*, we assume that the magnetic field intensity $\boldsymbol{H}$ is added continually by some mechanism below this region in the Corona. This part of the Corona temperature stays constant, within the resolution of our observations, possibly because of losses mainly due to irradiation (by the matter in the Corona moving possible up), whose energy would be replenished with the influx of a new ***B***-field flux and matter from below.

This is a 3D Langmuir's magneto-matter state, with properties described in Hill, 1960 [23] for a 2D absorption theory of gas by a solid under the same conditions envisioned by Langmuir. Hence, we envision the presence of a 3D Langmuir's magneto-matter state in which matter has coalesced completely with the magnetic field, whereas gas in the system is present, as described in the outline below, in which we use Berdichevsky and Schefers, 2015 [21] to assume:

1) Each height layer corresponds to the same value β. For this assumption to hold it is simpler to suppose that most matter is ionized, and we can assume this plasma is neutral, with most of it frozen to the dominant magnetic field. This is so despite the fact we are aware of that the plasma in the corona could possess $\beta \sim 1$, although $\gamma \ll 1$;

2) That there is in the solar corona an ideal gas of electrons, as is common in many circumstances, even when dealing with an electron gas in the conduction band of a solid metal, see e.g., Ziman, 1960 [24];

3) The equation of state of the gas of electrons represented by Equation (5) results from a system that is in thermal equilibrium. And because of the considered dimensions and assumptions, we consider three relevant works to which this electron gas may be subjected;

a) e-gas work (*i.e.,* $P_e dV$);

b) Gravitational work which the gas of electrons performs;

c) Magnetization work, like the one postulated in "magneto matter" in Berdichevsky and Schefers, 2015 [21].

The 1st through 3rd assumptions explains the validity of the relationship derived in Rodríguez Gómez, 2017 [19]. Same as was presented in Berdichevsky and Schefers, 2015 [21], for our study of the properties of the medium (magnetized-matter in a FR studied in-situ at 1 AU). We propose a 3-D Langmuir amorphous lattice as Langmuir proposed to explain adsorption of a gas by a solid's surface (e.g., Langmuir, 1916 [25], 1932, Langmuir and Taylor, 1932 [26]).

At 1 AU we refer to the interpretation of observations which are well documented, see e.g., Osherovich *et al.,* 1993 [27], 1997 [28], 1998 [29], Farrugia *et al.*, 1995 [30], Sittler and Burlaga, 1998 [31]. They show how, at different distances from the Sun, there is the occurrence of a similar anomalous behavior of the electron gas, *i.e.*, $\gamma < 1$.

See above-mentioned thermodynamics interpretation by Berdichevsky and Schefer, 2015 [21].

From the observations, we further assume that the Sun corona region is in the presence of an ensemble of uniformly magnetized matter. This "*unit element*" is a homogeneous tube of magnetized matter with a current, that flows along the magnetic field contributing to the generation of magnetization in the e-gas. Also, we assume "*no*" matter flow, but except for the current carrier(s) as postulated in the "1st" of "3" assumptions in this subsection (A simple estimate in Appendix

2 gives ~ 10^{13} "*micro*" magnetic-matter tubes with average width/length of 20 km/80 km in the Sun's corona region from 1.16 to $1.23R_{\odot}$. The ensemble number of the homogeneous tubes increases to 10^{15} when we consider the corona volume from 1.13 to $1.30R_{\odot}$).

Notice that the physics of our approach enables vibration of the above defined "*micro*" magneto matter tubes "*due to the breathing mode*," which would enable thermal conduction. This way, a thermal bath for the ensemble is assumed of the above-defined *tubes-ensemble* of magneto-matter. Hence, we consider it is possible to generate the global thermodynamic equilibrium.

Thus, we assume that the quiescent Sun Corona corresponds to a very long-lasting time-interval where it may be composed of an ensemble of homogeneous domains with gradually expanded extension in altitude between 1.1 and $1.3R_{\odot}$ in thermal equilibrium, following the scaling law

$$l_i = ¢(r_i - r_b) + l_b$$

where we assume $r_b = 20\ \text{km}$ and ¢ is a parameter to be adjusted, which will allow an expansion/reduction of *l* with the altitude interval of consideration in this study (see **Appendix 3**). Our "ensemble-unit" is the mean unit of volume of magnetized-matter in the corona. This mean unit is assumed to be magnetized matter in a tube of length $4l_i$ with magnetic field ***B*** along the tube axis, with current density ***J*** (// ***B***), and cross-section πl_i^2. The index "*i*" stands for each of the layers in altitude in the Corona considered in this study. It is assumed that there is no matter flow between these tubes of magnetized matter, which are considered to populate the quiescent Corona in the region of study (except perhaps only for the free flow of the current carriers). The stated assumption allows us to propose the following two possible thermodynamic conditions as physical understandings of the accurate description of the model of temperature and density of electrons in the low K-Corona, see also Rodríguez Gómez, 2017 [19]. The considered geometric values are listed in **Table 1**.

1) Single phase condition

The interval from $1.1R_{\odot}$ to $1.3R_{\odot}$ was considered as part of the corona. Interpreted fundamentally as a "micro-canonical" ensemble (see e.g., 1st Chapter in Hill, 1960 [23]), *i.e.*, a close ensemble of the magnetic tube region, allows us to test the nature of magnetic fields *anker* at both ends in the solar corona as it is assumed to happen in scales of large transients, see e.g., Burlaga, 1995 [32], Marubashi, 1997 [33]. For information about the frame of a magnetic flux-rope's evolution, see also Berdichevsky, 2013 [34], Berdichevsky, Lepping and Farrugia, 2003 [35]. This appears to be in consistent agreement with the model's evaluation of the magnetic field ***B*** in this region of the "low" Sun Corona, see **Table 2**. When there is no mixing between the frozen electrons in the magnetic field electrons, *i.e.*, the e-lattice, and the gaseous electrons, following (3a), (3b) and (3c), it is possible to write for the e-gas

$$PV = N_{mol}RT \tag{7a}$$

Table 2. Results for October 1-5, 2008, near extended solar minimum. The ± sign separates the *mean value* from variability in the interval used to compare the model to theory (thermodynamic interpretation).

Height ($r/R_\odot$)	1.16	1.19	1.23
Magnetic field[1] $B_{model}(r)$[2]	0.632 ± 0.005	0.592 ± 0.005	0.500 ± 0.005
Magnetic field $B_{theory}(r)$[3]	0.768	0.730	0.683
Model electrons T[1]	1.665×10^6 K	1.665×10^6 K	1.665×10^6 K
Theory electrons T	1.665×10^6 K	1.665×10^6 K	1.665×10^6 K
Model electrons N_e (nro/cm^3)	$4.3 \pm 0.2 \times 10^7$	$3.6 \pm 0.2 \times 10^7$	$3.2 \pm 0.2 \times 10^7$
Theory (a) N_e	3.79×10^7	3.60×10^7	3.35×10^7
Theory (b) N_e	4.30×10^7	3.60×10^7	3.20×10^7

We know that for, the electron gas N_{mol} is equal to the number of moles, in volume V, and that one mole contains 6.022×10^{23} particles, as Avogadro's number of particles, see e.g., Zemansky, 1957 [36], see **Table 3**. R = 8.314 462 Joules K/moles is the Reynolds constant, and T_e *is* the temperature given by the model, see **Table 1**.

For the gravitation field we consider just changes in altitude measured at adistance from $\langle r \rangle = 1.19 R_\odot$, which gives

$$W_{Gravitation} = GM_{sun} N_e V m_e \left(r - \langle r \rangle \right) / \langle r \rangle^2 \tag{7b}$$

and on the right panel (**Figure 1**) for

$$W_{magnetization} = \mu \boldsymbol{H} \cdot \boldsymbol{m} \tag{7c}$$

For the thermodynamic equilibrium in a system heat bath, we use the isothermal branch for the expression describing the evolution of one mole in going from location 1 to location 2, see left panel **Figure 1**. Consequently, we can write the change in the internal energy of the gas, see e.g., Zemansky, 1957 [36], for a differential change in altitude in the Sun Corona

$$dU = \delta Q - PdV + \frac{GM_{sun} m_e}{\langle r \rangle^2 \left(r - \langle r \rangle \right)} + \mu \boldsymbol{H} \cdot d\boldsymbol{m} \tag{8}$$

Under the simple consideration that quiescent conditions of the solar minimum corona imply heat equilibrium ($\delta Q = 0$) between constantly added magnetic energy from the Sun interior equilibrated by the Sun Corona radiative/convective losses, and conservation of temperature (*i.e.*, $dU = 0$) for a dilute ideal e-gas we obtain

$$T_e = T_o \quad \text{(Constant, isothermal consideration)} \tag{9a}$$

[1]From Berdichevsky *et al.* 2022; 2020.
[2]Model B-pressure in Gauss, about 1.233 times values from Berdichevsky *et al.* 2022 and 2020.
[3]Anchor value.

Table 3. Homogeneous region (HomgR) magneto-matter estimated constitutive properties for $T = 1.66 \times 10^6$ K in Corona height layers i. Work evaluation is performed for a single magnetic close tube. This means a homogeneous magnetic-flux tube of cross-section πl_b^2 and length $4l_b$. For the bottom (b) layer, it is assumed to change in size as the tube moves 1st to the layer mean (m), and finally to top (t).

Layer (i)	Bottom (b)	~mean (m)	Top (t)
Height ($r/R_\odot$)	1.16	1.19	1.23
HomgR [Volume]	$4l_b \pi l_b^2$	$4\pi\left(l_b + ¢[r_m - r_b]\right)^3$	$4\pi\left(l_b + ¢[r_t - r_b]\right)^3$
HomgR [Section]	πl_b^2	$\pi\left(l_b + ¢[r_m - r_b]\right)^2$	$\pi\left(l_b + ¢[r_t - r_b]\right)^2$
HomgR e-number/cm^3	$N_b 4l_b \pi l_b^2$	$N_m 4\pi\left(l_b + ¢[r_m - r_b]\right)^3$	$N_t 4\pi\left(l_b + ¢[r_t - r_b]\right)^3$
HomgR number moles	$\frac{N_b 4l_b \pi l_b^2}{6.022\times10^{23}}$	$\frac{N_m 4\pi\left(l_b + ¢[r_m - r_b]\right)^3}{6.022\times10^{23}}$	$\frac{N_t 4\pi\left(l_b + ¢[r_t - r_b]\right)^3}{6.022\times10^{23}}$
$\ln\left(\frac{N_i/r_i^2}{N_b/r_b^2}\right)RT$	_	-3.377×10^6	-6.093×10^6
$W_g\left(r - r_b\right)[\mathrm{J}]$	_	-4.040×10^5	-8.092×10^5
$W_M\left(r - r_b\right)[\mathrm{J}]$ (Equation (21))	_	-2.973×10^6	-5.284×10^6

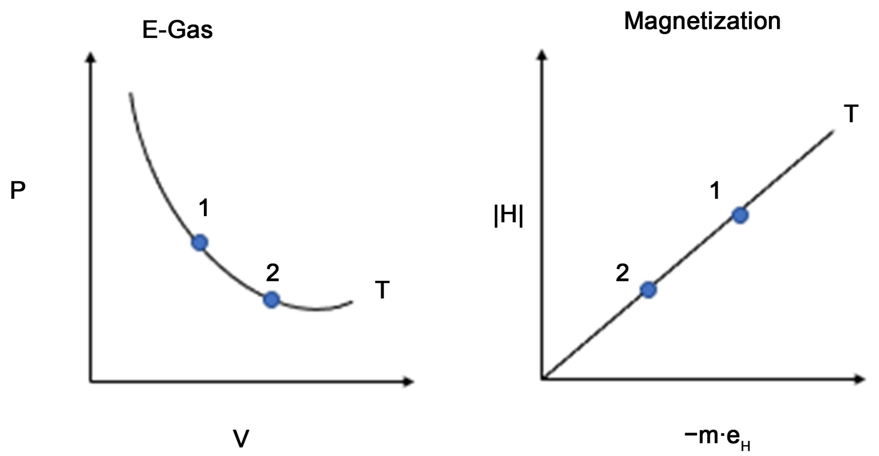

Figure 1. The isothermal branch of thermodynamic equilibrium in the system heat bath. Location 1 at r, and 2 at the incremental higher altitude "$r + \delta r$." Using arbitrary units, we illustrate the isothermal work conditions at a given height "h" on the e-gas by pressure and magnetic field changes as volume and magnetization change continuously.

$$N_e = N_o\left(\langle r\rangle/r\right)^2 \tag{9b}$$

The chosen distance $\langle r\rangle$, from the Sun-center, is convenient for comparing, in the figures, the model predictions with the one used in theory as shown in Table 2, where $r_o = \langle r\rangle = 1.19R_\odot$

In this case we can make an indirect estimate of the permeability of the model when we use a relationship

$$\frac{V_A(\mu)}{V_A(\mu_o)} = \left(\frac{\mu_o}{\mu}\right)^{1/2} \quad (10)$$

Compared to the estimated alfvenic speed at solar minimum at $1.19R_{\odot}$, using the prediction of the Alfvén from the estimated density, temperature, and magnetic field estimates, and in this way, we obtain $V_A(\mu_0) = 20 \pm 6\ \text{kms}^{-1}$.

We assume that medium will differ little from the conditions deeper near $1.08R_{\odot}$ in the corona from which there exists a good determination of EIT wave speeds. For the Alfvén speed of EIT waves, here values are taken from **Table 1** in Mann, *et al.* 1999 [37]. It is assumed that they constitute the non-compressible MHD mode (waves of the Alfvén-type) exited by the expulsion of the CME observed, *i.e.*,

$$V_A = \langle V_{EIT} \rangle = \frac{\sum_i V_{EIT}(i)}{n_{EIT}} \quad (11)$$

With $n_{EIT} = 16$ (a fewof 16 EIT waves associated with CMEs), in this case $\langle V_{EIT} \rangle = 207 \pm 18\ \text{km} \cdot \text{s}^{-1}$ is obtained. Therefore, we obtain the estimated permeability $\mu = 0.010 \pm 0.008\mu_o$ *i.e.*, it gives us a value of $\beta = 0.25 \pm 0.20$, smaller than one, surprisingly in qualitative agreement with a case study at 1 AU in Berdichevsky and Schefer, 2015 [21]. While **Table 2** shows that this result is reasonably in agreement with the model prediction, it is possible to speculate on a slightly less simple condition that would take care of the minor disagreements in *N* shown in **Table 1** between CODET model and Equations (9a) and (9b).

2) Two phases condition

The one-phase condition's description represents the corona electrons in possibly its most straightforward realization. However, one degree of complexity can be added. It is possible to suppose that, in the corona region between 1.1 and $1.3R_{\odot}$, there exists a thermodynamic interface between the "valence"-electrons and the "conduction"-electrons, where the conduction electrons constitute the e-gas. This is the condition of thermodynamic equilibrium of two electron phase states: the gas state increases with the volume as it occurs in the corona when transitioning from a lower altitude layer to a higher altitude one. An analogy can be made with the H_2O ice-water-vapor transition at $T = 275.16\ \text{K}$, when the isolated system undergoes a volume increase in the laboratory by a controlled quasi-stationary displacement of a piston, thereby increasing the volume of the thermally isolated container of the ice and its water vapor.

Closely related to the above discussed condition of energy conservation, Equation (8), is the condition of work equilibrium. This is the expression of the Helmholtz free energy *h*, *i.e.*,

$$d\left(h + PV + W_{Gravitation} + W_{magnetization}\right) = 0 \quad (12)$$

And considering that

$$h = \mu_{lattice} N_{lattice} + \mu_{gas} N_{gas} = \text{Constant} \tag{13}$$

i.e., we assume next that the thermodynamic phases (e-lattice and e-gas) are in equilibrium, where $\mu_{lattice}$, and μ_{gas}, constitute the chemical potential of each "e-state", *i.e.*,

$$VdP + dW_{Gravitation} + dW_{magnetization} = 0 \tag{14}$$

Once more, much as we did before for a single state case we may proceed similarly with *the* two-phase state. Hence, for the condition that we attempt to explain, the global Sun Corona model outlined in a region between 1.1 and $1.3\, r/R_\odot$, the two-phase condition in the particle density of Equation (13) allows us to write as a function of *r* the population for a dilute gas of electrons, the work equilibrium in the same form (Equation (7a))

$$PV = N_{mol} RT_e \tag{14a}$$

For the thermodynamic equilibrium in a heat bath, we use the isothermal branch to describe the evolution of one mole from location 1 to location 2, see the left panel in **Figure 1**.

For the gravitation field we consider just changes in altitude measured in distance *r* from the Sun, but centered at $\langle r \rangle = 1.2 R_\odot$, which gives Equation (7b)

$$W_{Gravitation} = GM_{sun} N_e V m_e \frac{r - \langle r \rangle}{\langle r \rangle^2} \tag{14b}$$

and on right panel (**Figure 1**) for the magnetic work (Equation (7c))

$$W_{Magnetization} = \mu \boldsymbol{H} \cdot \boldsymbol{m} \tag{14c}$$

In Equation (7c) we have the "intensive" thermodynamic variable $\boldsymbol{H}$ and the extensive variable $\boldsymbol{m}$, which can be written

$$\boldsymbol{m} = \boldsymbol{M} \Lambda \tag{15}$$

where Λ is the cross-section–perpendicular to the orientation of the dipole vector $\boldsymbol{m}$ *is* relevant to the problem. In our case, a layer located at any of the three altitude levels r_i in the Sun Corona is considered. Then at r_b the magnetic flux-tube cross-section is $1/4\pi l_b^2$ (see **Table 2**). The magnetization $\boldsymbol{M}$, a constitutive property of each material–when matter-homogeneity dominates-relates to $\boldsymbol{H}$, and $\boldsymbol{B}$ through

$$\boldsymbol{H} = \frac{\boldsymbol{B}}{\mu_O} - \boldsymbol{M} \tag{16}$$

and

$$\frac{\boldsymbol{B}}{\mu} = \boldsymbol{H} \tag{16b}$$

(Rationalized MKS system of units) see e.g., Jackson, 1963. We can write the differential work contribution as the magneto-matter displacement as a differential in height (*dr*) as

$$\frac{RTdP}{P} + \frac{GM_{sun} m_e}{r^2} dr - \mu \boldsymbol{H}(r) \cdot \boldsymbol{m}(r) dr = 0 \tag{17}$$

which gives for the integral of gravitational work

$$W_g\left(r-r_b\right)=\int_{r_b}^{r} GM_{sun}\frac{N_e V m_e}{r^2}dr \tag{18}$$

from $r_b = 1.16R_\odot$ to $r\,(r \le 1.23R_\odot)$.

In the case of magnetization work (Equation (7c)) we consider

$$\boldsymbol{M} = \alpha_m' \boldsymbol{H} \tag{19a}$$

i.e.,

$$\boldsymbol{m} = \Lambda\alpha_m' \boldsymbol{H} \tag{19b}$$

We use the expressions for $\boldsymbol{H}$ and $\boldsymbol{m}$ from Equation (19a) and Equation (19b) in the magnetic work expression (Equation (7c)) and use for the magnetic work the radial dependence suggested on the right panel in **Figure 1**. As noticed before, *i.e.*, Equation (19), we consider that each magnetic flux tube constitutes one element of the ensemble of magneto-matter in the quiescent Sun corona. Each of them has an inverse quadratic dependence with the distance of the magnetic flux-rope (flux-tube with twist) observed in-situ, see Berdichevsky, 2013 [34].

Hence, the magnetic work can be written as

$$W_m\left(r-r_b\right)=\int_{r_b}^{r}\mu\boldsymbol{H}(r)\cdot\boldsymbol{m}(r)\,dr=\int_{r_b}^{r}\mu\alpha_m'\Lambda\left|H\left(r_b\right)\right|^2 dr\Big/r^4 \tag{20}$$

when using the view of the representative magnetic field of the corona for one element in the ensemble of closed tubes of mean length 4*l* at layer b, while changing following with increasing distance, a simple proportionality $\left[\cent\left(r-r_b\right)+l\right]$ law change.

If the model provided isothermal conditions in the region of interest. We can further write the pressure evolution observed in the region of the Corona as

$$P\left(r-r_b\right)=P\left(r_b\right)\mathrm{e}^{-\frac{W_g\left(r-r_b\right)+W_m\left(r-r_b\right)}{RT}} \tag{21a}$$

using an ideal e-gas relation in Equation (7a), we can obtain

$$N(r)=N\left(\langle r\rangle\right)\left[\frac{r}{\langle r\rangle}\right]^2\mathrm{e}^{-\frac{W_g\left(r-r_b\right)+W_m\left(r-r_b\right)}{RT}} \tag{21b}$$

From Equation (21b) where a decrease in density with height as volume increase, adds the contribution of work, *i.e.*, the explicit role of the two-phase condition through the argument of the exponential function

$$W_g\left(r-r_b\right)=GM_{sun}N_e V m_e\left(r_b^{-1}-r^{-1}\right) \tag{22a}$$

as obtained from the integration of Equation (16), and

$$W_m\left(r-r_b\right)=\mu\alpha_m'\Lambda/3\left|H\left(r_b\right)\right|^2 l^4\frac{\left[\cent\left(r-r_b\right)+l\right]^3-l^3}{l^3\left[\cent\left(r-r_b\right)+l\right]^3} \tag{22b}$$

As obtained from the integration of Equation (20). Equation (22b) is valid for the *mean* size element of the ensemble in this two-phase approach of Sun K-Corona e-gas number density of the model for the three layers of the application of this model (the bottom one at $r_b = 1.16R_\odot$, the approximately mean one at $r_m = 1.19R_\odot$, and the top one at $r_t = 1.23R_\odot$), *i.e.*, we write

$$\ln\left(\frac{N_b/r_b^2}{N/r^2}\right)N_{mol}RT$$
$$= -\left\{GM_{sun}N_eVm_e\left(r_b^{-1}-r^{-1}\right)+\mu\alpha'_m\Lambda/3\left|H\left(r_b\right)\right|^2 l¢\left(r-r_b\right)\left(\left[¢\left(r-r_b\right)+\frac{3}{2l}\right]^2+\frac{3\left[\frac{l}{2}\right]^2}{\left[¢\left(r-r_b\right)+l\right]^3}\right)\right\} \quad (23)$$

with sub-index $i = b, m, t$, the variable r were replaced by r_i. where ¢ ≅ 2 × 10^{-5} *for* $¢(r_t\text{-}r_b) \sim l$, see **Appendix 3**. Henceforth, in **Table 4** the values for N_i, the gravitational work, and $\left|B_i^2\right|$ allows us the evaluation of the right hand-side of Equation (23) for the difference between layers *b, and m, as well asb and t*. The difference values are listed in **Table 3**, and in this case explicit consideration is given to the contribution of the gravitational potential.

In Equation (23) the unknowns are $|\boldsymbol{H}(r_b)|$ and the cross-section *time* magnetization coupling constant ($\Lambda\alpha'_m$). Using the constitutive relationship of the right in Equation (16) we obtain

$$\begin{aligned}\Lambda\alpha'_m &\cong -2.1\times10^6\ \text{Nmol/mol}\cdot\text{Joules}\Big/\left\{1/3\,\mu\left|\boldsymbol{H}\left(r_m\right)\right|^2\times0.65\times10^{10}\ \text{m}^2\right\} \\ &= -0.29\times10^{14}\,\mu\Big/\left[1/3\,B^2\left(r_m\right)\times0.65\times10^{10}\ \text{m}^2\right]\end{aligned} \quad (24)$$

With

$$\begin{aligned}1/3\,B^2\left(r_m\right)\times0.65\times10^{10}\ \text{m}^2 &= 1/3\left[0.7\times10^{-4}\ \text{Tesla}\right]^2\times0.65\times10^{10}\ \text{m}^2 \\ &= 6\left(\text{s/m}\right)^2\left[\text{Joule}/\left(\text{Coulomb/m}\right)\right]^2\end{aligned}$$

Then

$$1/3\,B^2\left(r_m\right)\times0.65\times10^{10}\ \text{m}^2 = 6\times10^{16}\Big/\left(4\pi\right)\mu_o\ \text{Joule} \quad (25)$$

We used the model value for T_e and the Sun radius $R_\odot$ in **Table 1**. In this way we obtain

$$\Lambda\alpha'_m \cong \mu/\mu_o\left[-0.29\times10^{14}\ \text{Joule}\Big/\left[0.5\times10^{16}\ \text{Joule}\right]\right] \quad (26)$$

and using Equation (16), the constitutive magnetic field relationship for a material, we can write

$$\mu/\mu_o = \left(1+\Lambda\alpha'_m\right) \quad (27)$$

with the value $\mu = 0.94\mu_0$ of the magnetic permeability of this thermo-dynamic state of the magnetized matter, considered with the help of the model's predictions for the three layers *i under consideration*, See **Table 3**.

These results are consistent with a polytropic adiabatic index smaller than 1 inferred in the model, with the parameters listed in **Table 1** Berdichevsky 2022 [4] and 2020 [5]. We notice that the properties of this quiescent magneto-plasma

Table 4. Magneto-matter constitutive properties for thermodynamic equilibrium, case "b" for the time interval from Jun. 1, 2008 to Jan 1, 2009. The cross-section relation between M and H is Λ (Λ = π10^8 m^2).

Case a. considering magnetization	with vacuum permeability μ_a
$\Lambda\alpha'_m$ (From model and estimated V_A)	−0.990
μ_a/μ_o	0.010 ± 0.008
$\langle\lvert\boldsymbol{B}\rvert\rangle$	0.703 × 10^{-4} Tesla
$\langle\lvert\boldsymbol{H}\rvert\rangle$	70.3 Ampere–turn/meter
$\langle\lvert\boldsymbol{M}\rvert\rangle$	−0.696 × 10^{-4} Tesla
nB (Magnetic Energy Density)	0.02 Joules (0.2 × 10^6 ergies)
Magnetic pressure with $\langle\lvert\boldsymbol{B}\rvert\rangle$ and μ_o	(50 ± 25) × 10^{-3} Nw/m^2
Plasma density ($\langle ion\ mass\rangle \sim 2m_p$)	1.27 × 10^{-14} kg/m^3
Matter pressure for $\langle T\rangle = 1.665\times10^6$ K	(3 ± 2) ×10^{-3} Nw/m^2
Plasma $\langle\beta\rangle < 1$	0.025 ± 0.020
Case b. considering magnetization	**with diamagnetic permeability μ_b**
$\Lambda\alpha'_m$ (*From consistent model evaluation*)	−0.06
μ_a/μ_o	0.94 ± 0.01
$\langle\lvert\boldsymbol{B}\rvert\rangle$	0.703 Gauss
$\langle\lvert\boldsymbol{H}\rvert\rangle$	0.745 Ampere–turn/meter
nB (Magnetic Energy Density)	0.00021 Joules (2.1 × 10^3 ergies)
$\langle\boldsymbol{J}\rangle$ (From model ***B***//***J*** assumption)	2.7 × 10^{-6} Ampere/m^2
Magnetic pressure (for $\mu_b/\mu_o = 0.94$)	0.5 ± 0.3 × 10^{-3} Newton/m^2
Matter pressure for $\langle T\rangle = 1.665\times10^6$ K	(3 ± 2) × 10^{-3} Nw/m^2
Plasma $\langle\beta\rangle > 1$ (for $\mu_b/\mu_o = 0.94$)	2.3 ± 0.2

matter do not appear to contradict the assumptions of the CODET model use of the PFSS magnetic potential field in the region of interest with magnetic permeability μ_0. In our view, nevertheless, the "model b" emphasizes that in the region of interest self-organization of an ensemble of each one of them takes place constituted by a magneto-plasma state inside a 3-D geometric shape of a tube with a current mostly aligned with the magnetic field present in this environment.

The derived nature of a diamagnetic medium is consistent with the properties found in an earlier interpretation made for entirely different conditions in Berdichevsky and Schefers, 2015 [21], which was one of strongly magnetized matter at 1 AU in the solar transient interval(s) amenable to the description of the magnetic flux-rope, *i.e.*, magnetic flux-field/tube with the Lundquist type of twist.

With the non-dispersive sound speed for the assumed magneto-matter structure, and using the information on the electron gas, it is possible to obtain the non-dispersive acoustic speed of the medium, see e.g., Myers, 1990 [38]

$$V_s = \left[\gamma K_B T_e / m_e\right]^{1/2} \tag{28}$$

which gives a value of V_s of approximately 2051 kms^{-1} - 2/3 × 10^{-2} *c*. It appears to agree with the lack of observed strong shock propagation in the interval between $1.1 - 1.3 R_\odot$, when its displacement (velocities) below ~1800 - 2200 kms^{-1}. On the other hand the medium would allow the formation slow shock with speed of ~300 kms^{-1} to propagate outward until it encounters conditions at higher altitudes (perhaps $r/R_\odot > 1.5 - 1.8$), where the system would become ***B***-field dominated, *i.e.*, $\beta < 1$, the Alfvénspeed would reach values of ~1700 kms^{-1} and the conditions would be set for the low solar corona shock to vanish. This has been earlier interpreted as being the case in the region, and here we follow the approach by Mann *et al.* 1999 [37] (see also Gopalswamy *et al.* 2001 [39]). They have assumed about one order of magnitude higher plasma density in a region closely below our careful re-evaluation for our value with "model b" of μ at r_b, see Equations (23) and (24) and the remote observations of N_e and T_e by e.g., Habbal *et al.* 2010 [40] (See **Appendix 4**, where we have followed the classical analysis of conditions of wave steepening, e.g., the tutorial about shocks by Kennel, Edmiston, and Hada, 1985 [41]. For a more up-to-date discussion through modeling see e.g., Hau and Wang, 2016 [42]).

Regarding the time to attain temperature equilibrium, we consider that a transport of an infinitesimal increment/decrement of heat ± δQ will occur close to the acoustic speed, Equation (28), see e.g., Landau and Lifshiftz, 1960 [43]. When we consider the collisional nature of heat in an ideal gas (in this case for the electrons), this implies for one ensemble unit of cross section $\Lambda = \pi(l/2)^2$ and length $4l$ that it will be equilibrate across (along) in ~10^{-2} s (4 × 10^{-2} s).

For the overall region of analysis from 1.16 to $1.23 R_\odot$ the expected equilibrium time will be about two to five times 150s, considering the non-homogeneous nature of the ensemble magnetized tubes related to the thermalization by collision, see **Table 4**.

Hence, we can estimate a few constitutive properties of the medium using MHD in the way of Berdichevsky and Schefers, 2015 [21], using our value for $|\boldsymbol{B}(r_b)|$ which the CODET model extends from the available measurement at the Sun Photosphere, see **Table 2**. Here, we used the ideal equation of the e-gas and the magnetized-matter assumption. An incomplete listing of the constitutive properties identified for the *magneto–matter steady state* interpretation here discussed of the quiescent solar corona is given in **Table 4**. Accounted errors in a few estimates listed in **Table 4** are based on explicit estimates of the observational uncertainties reported on temperature *T*, N_e, *B*, and other assumptions made, like the Alfvenic speed in the very low corona in the case of the *model a*.

4. Some Perspectives about the Unusual Hot State of Matter in the Sun Corona

Our approach in the previous section touches on a simple, consistent, physically well-grounded explanation for how a steady state of magneto–matter can exist in such a way that a steady high temperature in a quiescent Sun corona occurs. However, the presented interpretation (so far) does not touch on the continuous energy source needed to make such a phenomenon possible. The long-term stability observed for this thermal equilibrium in the quiescent Sun corona over a very long interval of time, like it is a solar minimum. We considered here an even more extended quiescent state of the Sun corona, in the Solar Cycle 23 - 24 minimum, which was composed of an interval of nearly two years of extremely low solar activity starting in 2008 and lasting till almost the end of 2009. A possible energy source in the form of matter and the magnetic field is briefly mentioned next.

We favor a recently developed view of the energy supply sustaining the heat we model in the low Sun corona. De Pontieu *et al.*, 2007 [15], suggesting that the spicules Type II may be key to the corona heating, put this mechanism forward. This is so because the spicules Type II appear to replenish the Sun corona steadily with both the magnetic field and plasma from under the Sun atmosphere/corona. It provides magnetic field and matter that is needed to sustain the energy of the system in a quasi-steady-state required in the magnetization-matter state interpretation. Because the Sun corona is an energetically open system with steady energy loss through radiative, and convective processes. Moreover, this mechanism appears promising when we consider that a by-product of the CODET model quantitative, the e-gas possesses an anomalous polytropic index much lower than one (see discussion of Equation (5) in Section 2).

A view of the Sun corona different from the one *we assume in this work* for the quiescent K-Corona is proposed in Bingham *et al.* 2010 [44]. It is for this environment that they develop a battery of wave-particle interaction possibilities well supported by plasma theory. Having the capability of heating to extremely high temperatures a region containing the largest magnetic fields, *i.e.*, one or more large active regions (ARs). In these ARs it is possible that the so-called, Shukla plasma waves (by Bingham et al named) make a substantial contribution to the extreme heating observed, see e.g., dispersive shear Alfvén waves (Gekelman, 1999 [45]), their possible ponderomotive force effects (Shukla *et al.*, 2004 [46]), and modulated polarized dispersive Alfvén waves in Bingham *et al.* 2010 [44], nonlinear effects in the interaction between clusters of dispersive Alfvén waves in studies by Sundkvist *et al.* 2005 [47], as well as zonal flows by kinetic Alfvén waves coupling, see Sagdeev *et al.*, 1978 a,b [48], Shukla 2005 [46].

The subject of application of the Bingham *et al.* 2010 [44] approach combined with the assumption of high non-collisional heat conductivity is introduced in connection to active region loop(s). While in our case methodically discussed, we observe a quiescent K-corona to which our thermodynamic assumptions of (approximate) equilibrium appear to be more adequate. Hampered by a lack of in-situ observations at the transition region of the mostly neutral solar region constituted by the photosphere/atmosphere of the Sun, the low matter density (for electrons a value of $N_e \sim 10^{14}$) has been hard to distinguish from between a variety of mechanisms for the heating of the solar atmosphere in its transition from the photosphere up to higher regions, first from the chromospheres and above it, and the TR, the much less populated, optical-thin region of the quiescent solar corona.

Alist of interesting possible mechanisms for the strong heating of the Sun's atmosphere in passing from the lower altitude region of the photosphere to the higher location of the chromosphere is proposed by Goodman, 1992 [49], 1993 [50]. The mechanism presented is based on a medium amenable to its description in terms of a resistive MHD model that dissipates in heat in the presence of waves, causing a strong temperature to increase in altitude between the two regions below the corona.

In the corona nano-flare heating mechanism is the proposed process for the Sun's corona gaining 1 - 2 million degrees Kelvin. It would be through nano-reconnection processes continuous in space and time in a fluid state with an e-gas with normal polytropic index $\gamma = 5/3$. In this model the fundamental heating mechanism, nano-flares, is the result of (nano) reconnections taking place approximately from the base of the Sun corona. Covering a region that extends over a similar altitude range comparable to the one explored in this work for the quiescent Sun corona with the CODET model. The observations of line widths (*i.e.*, non-thermal velocities) of ions do not appear to reflect the predicted non-thermal component in the plasma due to this postulated reconnection mechanism (nano-flares), which due to the optical thin nature of the quiescent corona is solely possible to observe at boundary regions of coronal magnetic holes (and/or AR). Itslacks observational support is discussed with technical detail in Brooks and Warren, 2016 [51].

Concerning the mechanism for heating the Sun corona, we mention here that besides the dissipation of waves energy which Bingham *et al.*, 2010 [44] suggested, other mechanisms will work there. It could be applied successfully in a scenario of the Sun corona and ARs. Furthermore, other authors have proposed wave generation of heat to help explain the coronal heating. These electromagnetic waves heating mechanism was first introduced in the 1950's by Schatzman, see e.g., Isenberg, Lee, and Hollweg, 1999 [52] (see also Isenberg and Hollweg, 1982 [53]). However, it has shown limited observational evidence as an explanation for the wave energy dissipation picture for its existence, e.g., Kasper, Lazarus, and Gary, 2008 [54]. Nevertheless, this view has been further elaborated with the addition of turbulence considerations in the process of particle acceleration (For a description of this mechanism, see e.g., Dmitruck, *et al.*, 2003 [55]). Notice that turbulence, which would obscure the wave activity at the Corona basis, could help explain the lack of detection of the intense wave activity required for the heating needed by a few million-degree corona temperatures.

The presence of alfvénic waves, of a various kind, is indeed observed all over the heliosphere up to ~9 AU from the Sun or even further away and supports this mechanism of the Sun corona heating. Observations in-situ reveal the fundamental alfvénic nature of the heliospheric medium, including the solar wind beginning with the in-situ observation of the Helio mission which covers from 0.28 to 1.0 AU, see e.g., Schwenn and Marsch, 1990 [56]. They failed to materialize the signatures of such intense MHD wave activity in the base of the low Sun quiescent corona. These observational failures cast doubts on the validity of these ideas of heating. Also, missing is the theoretically predicted non-thermal widening of the ion particle distributions predicted by the proposedwave-generated heating solution in the Sun corona regions here. See the detailed discussion on this subject in Brooks and Warren, 2016, and references therein.

5. Discussion

We used the magneto-matter tubes as a theoretical representation. It possesses a length scale l = 20 km. These tubes are a mathematical/theoretical simplifying tool that appears to be well supported by extrapolation to the low corona from observations both at 1 AU (Berdichevsky and Schefers, 2015 [21]) and near the Sun (also, May 2019 private communication by Alzate). This ensemble analysis allows us to build the unit block on which we assumed the *magneto-matter state* of the quiescent Sun's corona exists. In this way, we used statistical mechanics to estimate a few constitutive properties of the *magneto–matter steady state* that occupies the region of the Sun's corona $1.1 < r/R_{\odot} < 1.3$ regions.

At the center of our results is the determination of an estimated value for the diamagnetic permeability of the medium, along with other properties listed in **Table 4**. These *magneto matter* properties listed in **Table 4** correspond to a state of matter that satisfies the ideal–MHD conditions. Hence, the medium preserves magnetic flux, *i.e.*, helicity, which appears to be, most likely, an observationally property of the medium. See e.g., Antiochos, 2013 [57] discussion on the subject.

Regarding the time of equilibration implied in our description of *magneto–matter state*. We notice that it is consistent with the Ansatz made on the thermodynamic state of equilibrium of the quiescent sun corona at solar minimum.

When a short break of these quiescent conditions after a relatively short time-lapse interval order of magnitude comparable to the microscopic/macroscopic equilibration times of second fraction/minutes.

It is consistent with the observation indicating that it appears to be, in most cases, when the solar corona quickly recovers compared to the previous existing equilibrium condition(s).

The manifestation of a coronal slow forward shock appears consistent with metric Type II remote observations in the low Sun Corona in our region of interest with a plasma $\beta > 1$. On the other hand, only the very fast shocks with speeds of more than 1500 kms^{-1} in the time of the solar minimum here studied as a function of $r/R_{\odot}$ would propagate further from this coronal region into the heliosphere. This is the result of the observations, and its validation of low-density regions, dramatically reduce to one order magnitude less what was estimated in earlier works. The intensity of the magnetic field intensity also shows a decrease, but only by a factor less than two, see earlier studies, e.g., Saito, Poland, and Munro, 1977 [58].

We proposed that there is in the Sun's corona a *steady-state of magneto-matter* that appears to quantitative reproduce well the successful CODET model of the estimated electron density and temperature in the low solar corona extending in radial distance $1.1 < r/R_{\odot} < 1.3$ for the quiescent conditions. This is our Ansatz, an *amorphous* 3-*D Langmuir lattice* constituting a magneto-matter state in thermodynamic equilibrium (Berdichevsky and Schefers, 2015 [21], see also e.g., Langmuir, 1932 [59], 1934, Alfven, 1942 [60]). These ideas support the presence of magnetization-work, which in this case the CODET model allows for, providing a polytropic anomalous index $\gamma \sim 1/6$.

In our analysis it is worth seeing if we can re-interpret this perspective from a chemistry approach, see e.g., Robitaille, 2013 [61] in which a discussion is proposed based on the extreme acidity of the medium as conveyed by spectroscopic remote observation. See in this regard the pioneering, transformative work on the field of chemistry by Pauling, 1960 [62] (and for a physics perspective of a solid state of matter Ziman, 1960 [24]). There, in a series of works, Robitaille argues that the plain gas interpretation cannot hold, and the coalescence of a particular kind is attributed to be present, which is viewed as likely requiring extremely low temperatures for a few to a fraction of degrees Kelvin, assuming laboratory conditions and matter for which magnetic field condition(s) donot play a central role.

It is interesting here to point out that in this work we can agree with the freezing of most of the matter, when a hot magneto-matter state with a *simple* 3-D Langmuir amorphous lattice state nature (Berdichevsky and Schefers, 2015 [21]) is considered. A possibility is that anomalous e-gas in our coalescent *magneto matter state* could correspond with the valence electrons. In contrast, the particles carrying the current could be interpreted as the ones constituting the conduction(s) band(s) of their proposed unusual, extremely high acidity chemical manifestations of the Sun corona optical-spectra studies.

With regards to the particle population of the region of the corona considered, it is highly relevant to point out that only a fraction of it (less than ~ $1/15^{\text{th}}$ of the matter contained in the solar corona, estimated by the CODET model) becomes the solar wind, as observed in-situ from near 0.28 AU from the Sun center and beyond, *i.e.*, about 10 e/cm^3 at 1 AU. For this result, our view is consistent with the generalized one in which most of the matter does not escape the quiescent solar corona. This is a central subject to the geophysical space community and part of the distinction frequently made between two Solar corona regions, the one with "open" and the another with "closed" field lines. Here we have addressed the "closed" magnetic field region corona. The Solar Probe mission's current and future observations will test these views closer to the Sun (up to 0.1 AU or less).

It is worth considering how intriguing is that there is almost total heat insulation between the quiescent Sun corona and other structures present at contiguous places at the same height above the photosphere in the altitude range from about 1.12 to 1.25 $R_{\odot}$. It is also worth mentioning that for long-standing quiescent intervals, beyond hours, even days if not months of observed apparent equilibrium occurred side by side with much cooler prominence/hotter AR that defy understanding. *Id est*, they appear to corroborate that the sound derivations by Spitzer, 1956 [63] of heat conductivity in a magnetized plasma, as well as the more detailed derivations of Braguinskii, 1965 [64] do not to apply. Either we observe magnetized plasma regions hermetically and thermally insulated from each other or more cumbersome conditions exist. One such condition could involve some cooling mechanism that would involve heat (and possibly also matter) transport, keeping huge temperature differences in neighbor regions. As pointed out by Withbroe in 1988 [7], this is a circumstance that we still fail to understand.

Although we argue for spicules type II as a possible energy source responsible for keeping the temperature of the Sun quiescent corona at 1 to 2 million degrees, identifying with any certainty its source is outside the scope of this work. This is the case, as well, for several other areas here introduced which require further investigation, e.g., the estimate of the value of the chemical potentials of the valence and conduction electrons of the medium, our assumption that enables a quite satisfying evaluation of the permeability of this diamagnetic medium, see paragraphs above, and its value listed in **Table 4**. The study of some/several of these unknowns will eventually be performed elsewhere.

6. Conclusions

This work discusses for first time the medium structure and its interpretation as a novel state of matter. It will be considered and explored in the laboratory and in the natural environment, *i.e.*, the solar corona. We present a thermodynamic interpretation explaining the quantitative description of the CODET model results for the temperature and density of the free electrons in the low Sun corona (Berdichevsky *et al.*, 2022 [4]). In the following list, we indicate the main results.

- We tested the thermodynamic picture of a *magneto-matter steady state* hypothesis of a Langmuir 3D amorphous lattice consistent with the interplanetary plasma theory postulated by Alfvén for plasma freezing by the magnetic field for low-beta plasma conditions (see e.g., Alfvén, 1942 [60]). Here, the assumption is successfully tested for the case in which the CODET model shows an anomalous polytropic index when adjusted to achieve an optimal description of the quiescent Sun corona, a dominating feature in solar cycles near the solar minima.

- We emphasize that the physical arguments used are consistent with the explanation given for the anomalous nature of the polytropic index of the electron gas of the Sun K-corona. Indeed, an extremely low value $\gamma \ll 1$, is needed,(e.g., Rodríguez Gómez, J. M., (2017) [19]) for the CODET model solution to achieve quantitative agreement with observations. However, the solar minimum optimal CODET model choice provides quantitative results for N_e, and T_e (Berdichevsky *et al.* 2022 [4] **Table 1**).
- The smaller than one value of the polytropic index in the CODET model solution added to our physical interpretation gives credence to the claim that the spicules type II plays a relevant role in the Sun corona heating proposed by De Pontieu *et al.*, 2009 [65], 2011 [66].
- Our analysis is also consistent with the view that: 1) The potential magnetic field which decay with distance with the 3rd power of the ratio of the distance to the sun radius to the in-situ observation location (*i.e.*, $R_\odot / R_{in\text{-}situ}$). This B-field value at 1 AU practically would have disappeared (would be 10^{-3} nT or less). 2) The magnetization or better called currents-generated B-field will decay much more slowly, possibly linearly, giving qualitatively the observed value of about 2 nT at 1 AU (see <***M***> value in **Table 4**), which, depending on the history of the magnitude B from the corona to 1 AU, may range between 0.5 and 5.0 nT. Further, the model view of an ensemble of homogeneous regions in the quiescent Sun low corona would be consistent with a ***B***-field highly inclined to the imaginary line connecting the Sun with an observer at 1 AU from the Sun. The slow SW predicted by our model would be oriented most of the time on the ecliptic plane, which is not too far from observation for the slow solar wind. Also, the model is consistent with the frequent encounter in the slow SW of magnetic deeps (magnetic holes in the common language used by the heliospheric community).
- We notice the apparent presence of almost total insulation of the quiescent corona of interest in this study from other structures at the altitude discussed in the study. The implication of this is that insulation takes place as noticed and that more is needed to understand that property, in which it is apparent that the nature of the magnetic field structure necessarily plays a central role.

Acknowledgements

We owe thanks to many coworkers in the division 670 of NASA/GSFC among which we here remember the help received from Karin Muglach for providing one of us with up-to-date review work on the observational understanding of the solar atmosphere as well as helping with the interaction to other colleagues/experts about the Sun's atmosphere. I further am very thankful for the patience shown by Peter Young through extensive conversations with him. Generous conversations and suggestions I received from Richard de Vore, James Klinchuck, about solar corona and irradiance. Spiro Antiochos for literature sugges-

tions onto the subject of heat conductivity in magnetized plasmas, and to Gopalswamy on the shock propagation conditions in the low Sun corona.

Conflicts of Interest

The authors declare no conflicts of interest regarding the publication of this paper.

References

[1] Howard, R.A., Vourlidas, A., Bothmer, V., Colaninno, R.C., DeForest, C.E., Gallagher, B., Hall, J.R., Hess, P., Higginson, A.K., Korendyke, C.M., Kouloumvakos, A., Lamy, P.L., Liewer, P.C., Linker, J., Linton, M., Penteado, P., Plunkett, S.P., Poirier, N., Raouafi, N.E. and Rich. (2019) Near-Sun Observations of an F-corona Decrease and K-Corona Fine Structure. *Nature*, **576**, 232-236. https://doi.org/10.1038/s41586-019-1807-x

[2] Aschwanden, M.J. (2019) New Millennium Solar Physics. Astrophysics and Space Science Library, Volume 458. Springer Nature, Berlin. https://doi.org/10.1007/978-3-030-13956-8

[3] Aschwanden, M.J. (2005) Physics of the Solar Corona. An Introduction with Problems and Solutions. 2nd Edition, Praxis Publishing Ltd., Chichester, 892 p.

[4] Berdichevsky, D., Rodríguez Gómez, J., Vieira, L. and Dal Lago, A. (2022) Validation of Novel Model for Identification of Thermal Conditions in the Low Corona. *Advances in Aerospace Science and Technology*, **7**, 52-84. https://doi.org/10.4236/aast.2022.71004

[5] Berdichevsky, D.B., Rodríguez Gómez, J.M., Vieira, L. and dal Lago, A. (2020) Thermodynamics Interpretation of Electron Density and Temperature Description in the Solar Corona.

[6] Rodríguez Gómez, J.M., Vieira, L., dal Lago, A. and Palacios, J. (2018) Coronal Electron Density, Temperature and Solar Spectral Irradiance during Solar Cycles 23 and 24. *The Astrophysical Journal*, **852**, Article No. 137. https://doi.org/10.3847/1538-4357/aa9f1c

[7] Withbroe, G.L. (1988) The Temperature Structure, Mass, and Energy Flow in the Corona and Inner Solar Wind. *The Astrophysical Journal*, **325**, 442-467. https://doi.org/10.1086/166015

[8] Sanchez-Diaz, E., Rouillard, A.P., Lavraud, B., Segura, K., Tao, C., Pinto, R., Sheeley, N.R.J. and Plotnikov, I. (2016) The Very Slow Solar Wind: Properties, Origin and Variability. *Journal of Geophysical Research*: *Space Physics*, **121**, 2830-2841. https://doi.org/10.1002/2016JA022433

[9] Vasquez, B.J., Farrugia, C.J., Simmunac, K.D.C., Galvin, A.B. and Berdichevsky, D.B. (2017) Concerning the Helium-to-Hydrogen Number Density Ratio in Very Slow Ejecta and Winds near Solar Minimum. *Journal of Geophysical Research*: *Space Physics*, **122**, 1487-1512. https://doi.org/10.1002/2016JA023636

[10] Burlaga, L.F., Ness, N.F., Gurnett, D.A. and Kurt, W.S. (2013) Evidence for a Shock in Interstellar Plasma: Voyager 1. *The Astrophysical Journal Letters*, **778**, L3. https://doi.org/10.1088/2041-8205/778/1/L3

[11] Richardson, J.D., Wang, C., Liu, Y.D., Šafránková, J., NĚmeČek, Z. and Kurth, W.S. (2017) Pressure Pulses at Voyager 2: Drivers of Interstellar Transients? *The Astrophysical Journal*, **834**, Article No. 190. https://doi.org/10.3847/1538-4357/834/2/190

[12] Cummings, A.C., Stone, E.C., Hikkila, B.C., Lal, N., Webber, W.R., Johannsson, G.,

Moskalenko, I.V., Orlando, E. and Porter, T.A. (2016) Galactic Cosmic Rays in the Local Interstellar Medium Voyager 1 Observations and Model Results. *The Astrophysical Journal*, **831**, Article No. 18. https://doi.org/10.3847/0004-637X/831/1/18

[13] Zhao, J., Kosovichev, A.G. and Sekii, T. (2010) High-Resolution Helioseismic Imaging of Subsurface Structures and Flows of a Solar Active Region Observed by Hinode. *The Astrophysical Journal*, **708**, 304-313. https://doi.org/10.1088/0004-637X/708/1/304

[14] Klimchuk, J.A. (2006) On Solving the Coronal Heating Problem. *Solar Physics*, **234**, 41-77. https://doi.org/10.1007/s11207-006-0055-z

[15] de Pontieu, B., McIntosh, S., Hansteen, V.H., Carlsson, M. and Schrijver, C.J. (2007) A Tale of Two Spicules: The Impact of Spicules on the Magnetic Chromosphere. *Publications of the Astronomical Society of Japan*, **59**, S655-S662. https://doi.org/10.1093/pasj/59.sp3.S655

[16] Raouafi, N.E., Patsourakos, S., Pariat, E., Young, P.R., Sterling, A.C., Savcheva, A., Shimojo, M., Moreno-Insertis, F., DeVore, C.R., Archontis, V., Török, T., Mason, H., Curdt, W., Meyer, K., Dalmasse, K. and Matsui (2016) Solar Coronal Jets: Observations, Theory, and Modeling. *Space Science Reviews*, **201**, 1-53. https://doi.org/10.1007/s11214-016-0260-5

[17] Zurbuchen, T.H., Schadron, N.A. and Fisk, L.A. (1997) Direct Observational Evidence for a Heliospheric Magnetic Field with Large Excursions in Latitude. *Journal of Geophysical Research*, **102**, 24175-24181. https://doi.org/10.1029/97JA02194

[18] Fisk, L.A. (1996) Motion of the Footpoints of Heliosphere Magnetic Field Lines at the Sun: Implications for Recurrent Energetic Particle Events at High Heliographic Latitudes. *Journal of Geophysical Research*, **101**, 15547-15554. https://doi.org/10.1029/96JA01005

[19] Rodríguez Gómez, J.M. (2017) Evolution of the Electron Density, Temperature Distribution in the Solar Corona during Solar Cycles 23 and 24. PhD Thesis, Instituto Nacional de Pesquisas Espaciais (INPE), São Paulo. http://urlib.net/8JMKD3MGP3W34P/3NCJQLB

[20] Vernazza, J.E., Avrett, E.H. and Loeser, R. (1981) Structure of the Solar Chromosphere. III. Models of the EUV Brightness Components of the Quiet Sun. *Astrophysical Journal*, **45**, 635-725. https://doi.org/10.1086/190731

[21] Berdichevsky, D.B. and Schefers, K. (2015) On the Thermodynamics and Other Constitutive Properties of a Class of Strongly Magnetized Matter Observed in Astrophysics. *The Astrophysical Journal*, **805**, Article No. 70. https://doi.org/10.1088/0004-637X/805/1/70

[22] Dirac, P.M.A. (1967) The Principles of Quantum Mechanics. 4th Edition, Cambridge U. Press, Cambridge.

[23] Hill, T.L. (1960) An Introduction to Statistical Thermodynamics. Addison-Wesley, Reading. https://books.google.com/books?hl=en&lr=&id=QttFDwAAQBAJ&oi=fnd&pg=PP1&dq=An+introduction+to+statistical+thermodynamics&ots=_P7AZsbyHP&sig=zuYFIxpJjHfWh_710mtRmB1YayI#v=onepage&q=An%20introduction%20to%20statistical%20thermodynamics&f=false

[24] Ziman, J.M. (1960) Electrons and Phonons. The Theory of Transport Phenomena in Solids. Clarendon Press, Oxford. https://books.google.com/books/about/Electrons_and_Phonons.html?id=_HEsAAAAYAAJ

[25] Langmuir, I. (1916) The Constitution and Fundamental Properties of Solids and

Liquids, Part I, Solids. *Journal of the American Chemical Society*, **38**, 2221-2295. https://doi.org/10.1021/ja02268a002

[26] Langmuir, I. and Taylor, J.B. (1932) The Mobility of Caesium Atoms Adsorbed on Tungsten. *Physical Review*, **40**, 463-464. https://doi.org/10.1103/PhysRev.40.463

[27] Osherovich, V.A., Farrugia, C.J., Burlaga, L.F., Lepping, R.P., Feinberg, J. and Stone, R.D. (1993) Polytropic Relationship in Interplanetary Magnetic Clouds. *Journal of Geophysical Research*, **98**, 15,331-15,342. https://doi.org/10.1029/93JA01012

[28] Osherovich, V.A., Fainberg, J., Stone, R.G., MacDowall, R.J. and Berdichevsky, D.B. (1997) Self-Similar Evolution of Interplanetary Magnetic Clouds and Ulysses Measurements of the Polytropic Index inside the Cloud. *Proceedings* 31*st ESLAB Symposium*, *Correlated Phenomena at the Sun in Heliosphere and in Geospace*, Noordwijk, The Netherlands, 22-25 September 1997, 171-175.

[29] Osherovich, V.A., Fainberg, J., Stone, R.G., FItzenreiter, R. and Viñas, A.F. (1998) Measurements of Polytropic Index in the January 10-11, 1997 Magnetic Cloud Observed by Wind. *Geophysical Research Letters*, **25**, 3003-3006. https://doi.org/10.1029/98GL00547

[30] Farrugia, C.J., Osherovich, V.A. and Burlaga, L.F. (1995) Magnetic Flux Rope versus the Spheromak as Models for Interplanetary Magnetic Clouds. *Journal of Geophysical Research*, **100**, 12293-12306. https://doi.org/10.1029/95JA00272

[31] Sittler, E.C. and Burlaga, L.F. (1998) Electron Temperatures within Magnetic Clouds between 2 and 4 AU: Voyager 2 Observations. *Journal of Geophysical Research*, **103**, 17447-17454. https://doi.org/10.1029/98JA01289

[32] Burlaga, L.F. (1995) Interplanetary Magnetohydrodynamics. International Series in Astronomy and Astrophysics, Vol. 3, Oxford University Press, Oxford, 272 p.

[33] Marubashi, K. (1997) Interplanetary Magnetic Flux Ropes and Solar Filaments, Coronal Mass Ejections. In: Crooker, N., Joselyn, J. and Feynman, J., Eds., *Geophysical Monograph Series* 99, AGU, Washington DC, 147-156. https://doi.org/10.1029/GM099p0147

[34] Berdichevsky, D.B. (2013) On Fields and Mass Constraints for the Uniform Propagation of Magnetic-Flux-Ropes Undergoing Isotropic Expansion. *Solar Physics*, **284**, 245-259. https://doi.org/10.1007/s11207-012-0176-5

[35] Berdichevsky, D.B., Lepping, R.P. and Farrugia, C.J. (2003) Geometric Considerations of the Evolution of Magnetic Flux Ropes. *Physical Review E*, **67**, Article ID: 036405. https://doi.org/10.1103/PhysRevE.67.036405

[36] Zemansky, M.W. (1957) Heat and Thermodynamics. McGraw-Hill Book Co., New York. https://www.goodreads.com/book/show/26257955-heat-and-thermodynamics--sie

[37] Mann, G., Aurass, H., Klassen, A., Estel, G. and Thompson, B.J. (1999) Coronal Transient Waves and Coronal Shock Waves. *Proceedings* 8*th SOHO Workshop* "*Plasma Dynamics and Diagnostics in the Solar Transition Region and Corona*", Paris, 22-25 June 1999, ESA SP-446.

[38] Myers, H.P. (1990) Introductory Solid-State Physics. Taylor and Francis, London. https://doi.org/10.1201/9781315273303

[39] Gopalswamy, N., Lara, A., Kaiser, M.L. and Bougeret, J.-L. (2001) Near-Sun and Near-Earth Manifestations of Solar Eruptions. *Journal of Geophysical Research*, **106**, 25261-25277. https://doi.org/10.1029/2000JA004025

[40] Habbal, S.R., Druckmüller, M., Morgan, H., Daw, A., Johnson, J., Ding, A., Arndt, M., Esser, R., Rusin, V. and Scholl, I. (2010) Mapping the Distribution of Electron

Temperature and Fe Charge States in the Corona with Total Eclipse Observations. *The Astrophysical Journal*, **708**, 1650-1662. https://doi.org/10.1088/0004-637X/708/2/1650

[41] Kennel, C.F., Edmiston, J.P. and Hada, T. (1985) A Quarter Century of Collisionless Shock Research. In: Stone, R.G. and Tsurutani, B.T., Eds., *Collisionless Shocks in the Heliosphere*: *A Tutorial Review*, AGU, Washington DC, 1-36. https://doi.org/10.1029/GM034p0001

[42] Hau, L.N. and Wang, B.-J. (2016) Slow Shock and Rotational Discontinuity in MHD and Hall MHD Models with Anisotropic Pressure. *Journal of Geophysical Research*: *Space Physics*, **121**, 6245-6261. https://doi.org/10.1002/2016JA022722

[43] Landau, L.D. and Lifshiftz, E.M. (1960) Electrodynamics of Continuous Media, Vol. 8 of a Course of Theoretical Physics. Translated from Russian by Sykes, L.D. and Bell, J.S., Pergamon Press Ltd., Oxford.

[44] Bingham, R., Shukla, P.K., Eliasson, B. and Stenflo, J. (2010) Solar Coronal Heating by Plasma Waves. *Journal of Plasma Physics*, **76**, 135-158. https://doi.org/10.1017/S0022377809990031

[45] Gekelman, W. (1999) Review of Laboratory Experiments on Alfvén Waves and Their Relationship to Space Observations. *Journal of Geophysical Research*, **104**, 14417-14435. https://doi.org/10.1029/98JA00161

[46] Shukla, P.K., Stenflo, L., Bingham, R. and Eliasson, B. (2004) Nonlinear Effects Associated with Dispersive Alfvén Waves in Plasmas. *Plasma Physics and Controlled Fusion*, **46**, B349. https://doi.org/10.1088/0741-3335/46/12B/030

[47] Sundkvist, D., Krasnoselskikh, V., Shukla, P.K., Vaivads, A. andre, M., Buchert, S. and Reme, H. (2005) *In Situ* Multi-Satellite Detection of Coherent Vortices as a Manifestation of Alfvénic Turbulence. *Nature*, **436**, 825-828. https://doi.org/10.1038/nature03931

[48] Sagdeev, R.Z., Shapiro, V.D. and Shevchenko, V.I. (1978) Excitation of Convective Cells by Alfvén Waves. *JETP Letters*, **27**, 340.

[49] Goodman, M. (1992) On Driven Dissipative, Energy-Conserving Magnetohydrodynamic Equilibria. *Journal of Plasma Physics*, **48**, 177-202. https://doi.org/10.1017/S0022377800016482

[50] Goodman, M. (1993) Driven, Dissipative, Energy-Conserving Magnetohydrodynamic Equilibria. Part II. The Screw Pinch. *Journal of Plasma Physics*, **49**, 125-159. https://doi.org/10.1017/S002237780001686X

[51] Brooks, D.H. and Warren, H.P. (2016) Measurements of Non-Thermal Line Widths in Solar Active Regions. *The Astrophysical Journal*, **820**, Article No. 63. https://doi.org/10.3847/0004-637X/820/1/63

[52] Isenberg, P.A., Lee, M.A. and Hollweg, J.V. (1999) A Kinetic Model of Coronal Heating and Acceleration by Ion-Cyclotron Waves: Preliminary Results. *Solar Physics*, **193**, 247-257. https://doi.org/10.1007/978-94-010-0860-0_16

[53] Isenberg, P.A. and Hollweg, J.V. (1982) Finite Amplitude Alfven Waves in a Multi-Ion Plasma' Propagation, Acceleration, and Heating. *Journal of Geophysical Research*, **87**, 5023-5029. https://doi.org/10.1029/JA087iA07p05023

[54] Kasper, J.C., Lazarus, A.J. and Gary, S.P. (2008) Hot Solar-Wind Helium: Direct Evidence for Local Heating by Alfvén-Cyclotron Dissipation. *Physical Review Letters*, **101**, Article ID: 261103. https://doi.org/10.1103/PhysRevLett.101.261103

[55] Dmitruck, P., Matthæus, W.H., Seenu, N. and Brown, M.R. (2003) Test Particle Acceleration in Three-Dimensional Magnetohydrodynamic Turbulence. *The Astrophysical Journal*, **597**, L81-L84. https://doi.org/10.1086/379751

[56] Schwenn, R. and Marsch, E. (1990) Physics of the Inner Heliosphere. Volumes I and II. Springer Verlag, Berlin. https://doi.org/10.1007/978-3-642-75361-9

[57] Antiochos, S.K. (2013) Helicity Condensation as the Origin of Coronal and Solar Wind structure. *The Astrophysical Journal*, **772**, Article No. 72. https://doi.org/10.1088/0004-637X/772/1/72

[58] Saito, K., Poland, A.I. and Munro, R.H. (1977) A Study of the Background Corona near Solar Minimum. *Solar Physics*, **55**, 121-134. https://doi.org/10.1007/BF00150879

[59] Langmuir, I. (1932) Surface Chemistry, Nobel Lecture, December.

[60] Alfvén, H. (1942) Existence of Electromagnetic-Hydromagnetic Waves. *Nature*, **150**, 405-406. https://doi.org/10.1038/150405d0

[61] Robitaille, P.-M. (2013) The Liquid Metallic Hydrogen Model of the Sun and the Solar Atmosphere V. On the Nature of the Corona. *Progress in Physics*, **3**, L30-L36.

[62] Pauling, L. (1960) The Nature of the Chemical Bond and the Structure of Molecules and Crystals, III. Cornell University Press, Ithaka. http://boscoh.com/pdf/pauling.pdf

[63] Spitzer, L. (1956) Plasma Physics. Interscience Tracts on Physics and Astronomy.

[64] Braguinskii, S.I. (1965) Transport Processes in a Plasma. Reviews of Plasma Physics, Volume 1. Authorized Translation from the Russian by Herbert Lashinsky, Consultants Bureau, New York.

[65] De Pontieu, B., McIntosh, S.W., Hansteen, V.H. and Schrijver, C.J. (2009) Observing the Roots of Solar Coronal Heating-In the Chromosphere. *The Astrophysical Journal*, **701**, L1. https://doi.org/10.1088/0004-637X/701/1/L1

[66] De Pontieu, B., McIntosh, S.W., Carlsson, M., Hansteen, V.H., Tarbell, T.D., Boerner, P., Martinez-Zycora, J., Schreiver, C.J. and Title, A.M. (2011) The Origins of Hot Plasma in the Solar Corona. *Science*, **331**, 55-58. https://doi.org/10.1126/science.1197738

[67] Kennel, C., Edmiston, J. and Hada, T. (1985) A Quarter Century of Collisionless Shock Research. In: *Collisionless Shocks in the Heliosphere*: *A Tutorial Review* (*A*87-25326 09-92), American Geophysical Union, Washington DC, 1-36. https://doi.org/10.1029/GM034p0001

Appendix 1

Using Equation (4) and assuming we are in the presence of a gas of electrons that behaves in an adiabatic process as an ideal gas with a polytropic index

$$\gamma = \zeta / \alpha$$

Which, with the values ζ and α in **Table 1**, gives a value of γ very close to 1/6, *i.e.*, quite anomalous since it is smaller than 1. Using Equation (4) in Berdichevsky and Schefers, 2015 [21], the anomalous polytropic index γ can be interpreted as related to the occurrence of two coupled works by the e-gas, *i.e.*, the usual "pdV" work associated with an ideal gas and a magnetization work "$\boldsymbol{B}\cdot d\boldsymbol{m}$"

Using the expression

$$\gamma = 1 + R/C_v - R/C_v \eta$$

in Equation (7), also in Section 2 of Berdichevsky and Schefers, 2015 [21] for the e-gas, and using $\gamma = 1/6$, it is straightforward to find the value for the coupling constant $\eta = 5/4$ between the two works in an adiabatic process (*i.e.*, $\eta = \boldsymbol{B}\cdot d\boldsymbol{m}/pdV$), e.g., during the passage of a non-dispersive pressure wave in the assumed 3D Langmuir magneto-matter steady-state in the Sun corona. It is further noticed that, for the considered ideal gas

$$T \propto N^{-1+\gamma}$$

an increase in density cools of the structure, which is an outcome of the $\gamma < 1$ anomalous nature of the medium.

Appendix 2

Here we look at the already derived in Berdichevsky *et al.* 2022 [4] and 2020 [5] (their **Appendix 1**) possible extension in volume of the quiescent solar corona between 1.16 and $1.23R_{\odot}$. Then, the volume value is

$$0.86(4\pi/3)\left(R_{top} - R_{bottom}\right)^3$$

where $R_{top} = 1.23R_{\odot}$ $R_{bottom} = 1.16R_{\odot}$. This volume region, when divided by the assumed mean tube structure corresponds to

$$\pi(l/2)^2 4l = 2.5\times10^{44}\ \text{km}^3$$

It gives an ensemble of mean homogeneous regions of 10^{13} elements. This value is good for statistical mechanics/thermodynamics study.

Appendix 3

Here we make the simplifying geometric assumption

$$¢\left(r - r_b\right) = (1.23 - 1.16)l$$

i.e.,

$$0.07¢R_{\odot} = 0.07l$$

Hence $¢ = l/R_{\odot}$

Appendix 4

As it is known, the wave mode propagations in MHD are the fast, intermediate, and slow. Here we follow the notation of Kennel, Edmiston, and Hada, 1985 [67], *i.e.*, for these MHD wave speeds we use C_i, *with* i = *Fast*, *Intermediate*, *Slow*, as well as C_S = *gas speed*, and C_A = *Alfven speed* respectively. Hence, we can write

$$2C_{Fast}^2 = \left\{ \left(C_A^2 + C_s^2 \right)^2 - \left[\left(C_A^2 + C_s^2 \right)^2 - 4C_A^2 C_s^2 \cos(\theta) \right]^{1/2} \right\}$$

$$C_{Intermediative}^2 = C_A^2 \cos^2(\theta)$$

$$2C_{Slow}^2 = \left\{ \left(C_A^2 + C_s^2 \right)^2 - \left[\left(C_A^2 + C_s^2 \right)^2 - 4C_A^2 C_s^2 \cos(\theta) \right]^{1/2} \right\}$$

where $\theta = \arccos\{\boldsymbol{B}_{up} \cdot \boldsymbol{n}_{Shock}\}$, *i.e.*, θ is the angle between the direction of the magnetic field upstream of the shock ($\boldsymbol{B}_{up}$) with the shock normal ($\boldsymbol{n}_{Shock}$). Further we notice that in this environment our models give $C_S^2 > C_A^2$. And the Kennel, Edmiston, and Hada analyses indicate that the *Slow-Shock* steepens fastest when $C_S^2 > C_A^2$, quickly generating a shock wave. We here refer to the condition in which $\theta \sim 0$, which is consistent with the geometry $\boldsymbol{B}$-field approximately parallel to the surface of the Sun, and physics of the occurrence of strong density fluctuation limit for a near parallel shock $\delta N \sim N$. *i.e.*, our problem appears consistent with the remote metric/decametric Type II radio burst observations interpreted commonly as manifestations of shocks near the TR in the low Sun corona *only*, soon after the CME starts, as it was argued in the past, see e.g., Gopalswamy *et al.* 2001 [39], Mann *et al.*, 1999 [37].